Low temperature fabrication of high performance and transparent Pt counter electrodes for use in flexible dye-sensitized solar cells

XIAO YaoMing, WU JiHuai[*], CHENG CunXi, CHEN Yuan, YUE GenTian, LIN JianMing, HUANG MiaoLiang, FAN LeQing & LAN Zhang

Engineering Research Center of Environment-Friendly Functional Materials, Ministry of Education, Institute of Materials Physical Chemistry, Huaqiao University, Quanzhou 362021, China

High performance Pt counter electrode is prepared by using vacuum thermal decomposition at a relatively low (120°C) temperature on a flexible polyethylene naphthalate substrate coated with indium-doped tin oxide for use in flexible dye-sensitized solar cells. The obtained Pt counter electrode shows a good chemical stability, high light transmittance, and high electrocatalytic activity for the I_3^-/I^- redox reaction. The energy conversion efficiency of a flexible dye-sensitized solar cell based on the prepared Pt counter electrode and a TiO_2/Ti photoanode reaches 5.14% under a simulated solar light irradiation with intensity of 100 mW cm^{-2}.

platinum, counter electrode, vacuum thermal decomposition, cyclic voltammogram, flexible dye-sensitized solar cells

Since the first prototype of a dye-sensitized solar cell (DSSC) was reported in 1991 by O'Regan and Grätzel, DSSCs have been aroused widely attention and research due to their low cost and simple preparation procedure. A DSSC with a photoelectric conversion efficiency of 12% have been achieved [1,2]. In general, a DSSC consists of a dye-sensitized porous nanocrystalline TiO_2 film electrode, a redox electrolyte, and a platinized counter electrode. Standard DSSCs, in which the porous titania films are mounted on rigid conductive glass substrates, suffer from a number of limitations. Flexible substrates, such as metal foils and polymer substrates, have attracted interest by overcoming these issues as they tend to be lighter, are impact-proof, and are made at a lower cost [3–7]. Flexible DSSCs can also be constructed using large-scale continuous production and rapid coating methods, which would further decrease the cost of DSSCs. The function of the counter electrode is to transfer electrons arriving from the external circuit back to the redox electrolyte and to catalyze the reduction of the triiodide ion [8–10]. Therefore, it is important to develop a simple and suitable method to produce a counter electrode on a flexible substrate which also exhibits good chemical stability and high electrocatalytic activity for the I_3^-/I^- redox process.

Pt counter electrodes on flexible substrates have been prepared by sputtering, electrochemical deposition or chemical reduction. Ikegami et al. deposited a Pt/Ti bilayer on a polyethylene naphthalate substrate coated with indium-doped tin oxide (ITO/PEN) using vacuum sputtering and the fully plastic DSSC had a conversion efficiency of 4.31% [11]. Grätzel electrodeposited Pt catalyst onto ITO/PEN to make a flexible DSSC with a conversion efficiency of 7.2% [12]. Kang et al. [13], Park et al. [14], and Chen et al. [15] used chemical reduction to prepare Pt counter electrodes. They spread an isopropanol solution of $H_2PtCl_6 \cdot 6H_2O$ on a conductive plastic substrate followed by reduction with $NaBH_4$. Sun et al. [16] also fabricated a Pt counter electrode using ethylene glycol reduction of $H_2PtCl_6 \cdot 6H_2O$ at 180°C.

Thermal decomposition of isopropanol solutions of H_2PtCl_6 has been widely used to prepare high performance

*Corresponding author (email: jhwu@hqu.edu.cn)

Pt counter electrodes because it gives a stable product with higher exchange current densities for the I_3^-/I^- couple [17]. However, this process requires a heat treatment at 400°C that most plastic substrates cannot bear. In this paper, to exploit the superiority of platinum, we report a facile vacuum thermal decomposition method at a low temperature to prepare the high performance platinum counter electrode on the flexible ITO/PEN substrate, which has good light transmittance for the TiO$_2$/Ti photoanode.

1   Experimental

1.1   Materials

H$_2$PtCl$_6$·6H$_2$O, ethanol, isopropanol, n-butanol, iodine, lithium iodide, lithium perchloratetetrabutyl, ammonium iodide, 4-tert-butyl-pyridine (TBP), acetonitrile (AN), tetrabutyl titanate, titanium tetrachloride, oxalic acid, nitric acid, PEG-20000 and Triton X-100 were purchased from the Shanghai Chemical Agent Ltd., Shanghai, China (Analysis purity grade). ITO/PEN (12 Ω cm^{-2}) was purchased from PECCELL Technologies Inc., Yokohama, Japan. The 0.03 mm Ti foil was purchased from Baoji Yunjie Metal Production Co., Ltd., Baoji, China. The N719 dye [*cis*-di(thiocyanato)-N,N'-bis-(2,2'-bipyridyl-4-carboxylic acid-4-tetrabutylammonium carboxylate) ruthenium (II)] was purchased from Solaronix SA, Switzerland. All agents were used without further purification.

1.2   Preparation of flexible Pt counter electrodes

The ITO/PEN substrate was submerged in a 50% aqueous ethanol solution for one day without ultrasonication, before being cleaned several times with absolute ethanol. It is important that the ITO/PEN substrate is not cleaned with strong acid or base, as this damages the substrate [18].

A typical Pt counter electrode was prepared by the following steps. H$_2$PtCl$_6$·6H$_2$O was dissolved in a 1:1 mixture of isopropanol and n-butanol at concentrations of 0%, 0.25 wt%, 0.50 wt% and 0.75 wt% [17]. The appropriate H$_2$PtCl$_6$·6H$_2$O solution was stirred for 6 h at room temperature and then sprayed onto the ITO/PEN substrate to give an electrode with an active area of 1.0 cm×0.6 cm. After blow-drying at room temperature, the substrates were heated at different temperatures and different times in a vacuum oven (Suzhou Jiangdong Precision Instrument Co., Ltd., Suzhou, China), to form the Pt counter electrodes. A commercial flexible counter electrode Pt/Ti was purchased from PECCELL Technologies Inc. for comparison.

1.3   Fabrication of flexible TiO$_2$ film electrodes

The Ti foil was used as a substrate for the nanocrystalline TiO$_2$ film to fabricate the flexible DSSC. Before use, it was washed with mild detergent and rinsed in distilled water, then immersed in saturated oxalic acid solution for 10 min before being rinsed with distilled water.

The TiO$_2$ colloid was prepared as follows. Tetrabutyl titanate (10 mL) was rapidly added to distilled water (150 mL), with a white precipitate forming immediately. The precipitate was filtered using a glass frit and washed three times with distilled water. The filter cake was added to dilute nitric acid (0.1 M, 1 M=1 mol L^{-1}, 120 mL) with vigorous stirring at 80°C until the slurry became a translucent blue-white liquid. The resultant colloidal suspension was autoclaved at 200°C for 12 h to form a milky white slurry. This was then concentrated to one-quarter of its original volume, and PEG-20000 (10 wt% slurry) and a few drops of emulsification regent (Triton X-100) were added to form the final TiO$_2$ colloid.

The TiO$_2$ colloid was coated onto the Ti foil using a doctor-scraping technique. The thickness of the TiO$_2$ film was controlled by the thickness of the adhesive tape around the edge of the cleaned Ti foil [19–21]. After drying at room temperature, the TiO$_2$ thin films were sintered at 450°C for 30 min in air to give nanocrystalline TiO$_2$ films. The TiO$_2$ electrodes were cooled to 80°C and immersed in a 0.05 M TiCl$_4$ solution for 6 h, before being washed three times with distilled water. The treated TiO$_2$ films were again sintered at 400°C for 20 min. On cooling to 80°C, the flexible TiO$_2$ films were immersed in a 2.5×10^4 M solution of dye N719 in absolute ethanol solution for 24 h to adequately absorb the dye to finally give the flexible dye-sensitized TiO$_2$ film electrodes.

1.4   Assembly of flexible DSSCs

Figure 1 shows a flexible DSSC. The flexible DSSC was assembled by injecting the redox electrolyte into the gap between the TiO$_2$ film electrode (anode electrode) and a Pt counter electrode. The two electrodes were clipped together and a cyanoacrylate adhesive was used to prevent the electrolyte solution from leaking. Epoxy resin was used to further sealing the cell to ensure the stability of the cell. The injected redox electrolyte consisted of 0.60 M tetrabutyl
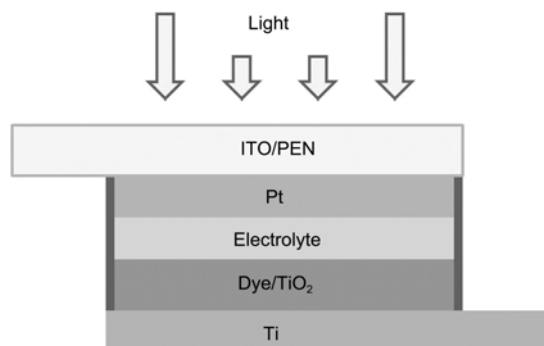

Figure 1   Schematic diagram of the flexible DSSC.

ammonium iodide, 0.10 M LiI, 0.10 M I_2, and 0.50 M 4-tert-butyl-pyridine in acetonitrile.

1.5   Characterization

The surface features and elemental composition of the flexible Pt counter electrode were observed using a scanning electron microscope (SEM, Hitachi S-4800, Japan) and an energy-dispersive X-ray spectrometer (EDS) attached to the SEM. The cyclic voltammetry (CV) was measured in a three electrode electrochemical cell with an Electrochemical Workstation (CHI660C, Shanghai Chenhua Device Company, Shanghai, China) using the Pt counter electrode as the working electrode, a Pt-foil as the counter electrode, and Ag/AgCl as the reference electrode in an acetonitrile solution of 10 mM LiI, 1.0 mM I_2 and 0.10 M $LiClO_4$. CV tests were performed at scan rates of 20–200 mV s^{-1}.

1.6   Photoelectrochemical measurements

The photovoltaic performance test of the flexible DSSC measured the *J-V* character curves using the CHI660C workstation under irradiation with simulated solar light from a 500 W xenon arc lamp (XQ-500W, Shanghai Photoelectricity Device Company, Shanghai, China) in ambient atmosphere. The incident light intensity was 100 mW cm^{-2} (AM 1.5) and the active area of the flexible DSSC cell was 0.8×0.4 cm^2. The photoelectronic performances (i.e., fill factor (*FF*) and overall energy conversion efficiency (η)) were calculated by the following equations [22]:

$$FF = \frac{V_{max} \times J_{max}}{V_{OC} \times J_{SC}}, \qquad (1)$$

$$\eta(\%) = \frac{V_{max} \times J_{max}}{P_{in}} \times 100\% = \frac{V_{OC} \times J_{SC} \times FF}{P_{in}} \times 100\%, \quad (2)$$

where J_{SC} is the short-circuit current density (mA cm^{-2}), V_{OC} is the open-circuit voltage (V), P_{in} is the incident light power, and J_{max} (mA cm^{-2}) and V_{max} (V) are the current density and voltage in the *J-V* curves, respectively, at the point of maximum power output.

2   Results and discussion

2.1   Morphology and compositions of the Pt counter electrode

Figure 2(a) and (b) show the SEM images of the Pt counter electrodes at different magnifications. The Pt particles are well dispersed on the transparent ITO/PEN substrate with a diameter of about 100–200 nm. The surface of the electrode has a large amount of void space, allowing high light transmittance. When hydrated H_2PtCl_6 is heated at 120°C for 2 h in a vacuum, it decomposes as follows: $H_2PtCl_6 \cdot 6H_2O \leftrightarrow PtCl_4 + 2HCl + 6H_2O$; $PtCl_4 \leftrightarrow PtCl_2 + Cl_2$; $PtCl_2 \leftrightarrow Pt + Cl_2$.
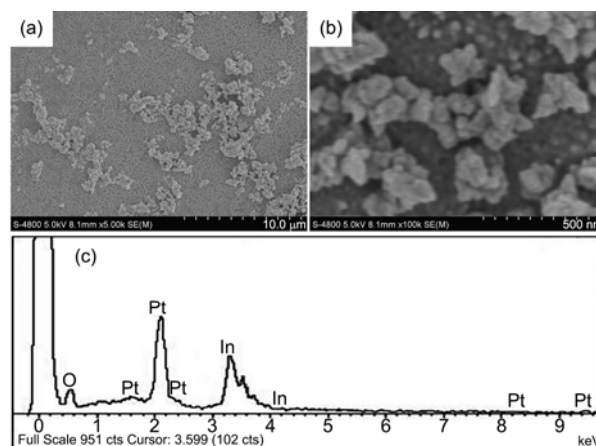

Figure 2   SEM images (a), (b) and EDS spectrum (c) of the flexible Pt counter electrode.

Although all three reactions are reversible, they produce gaseous products, and the vacuum drives the reaction forward with their removal. According to the EDS spectrum (Figure 2(c)), which shows that the Pt counter electrode consists of Pt, In and O, the H_2PtCl_6 has completely decomposed at the low temperature in the vacuum oven.

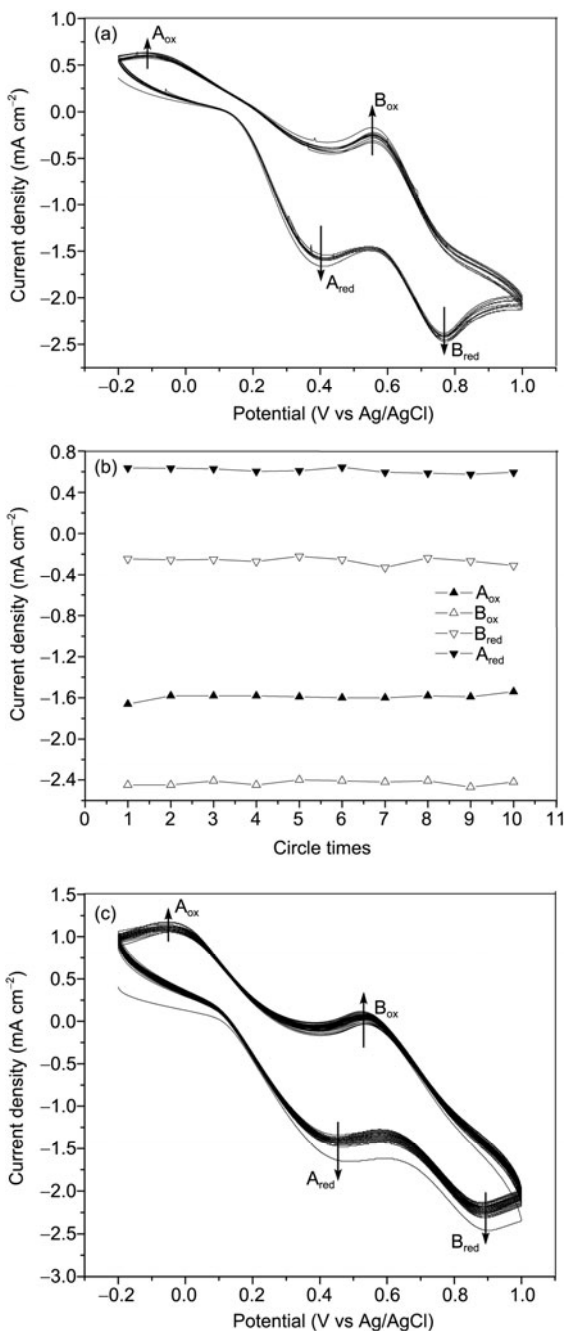### 2.2   Electrochemical properties of the Pt counter electrode

Figure 3 shows cyclic voltammograms for a ITO/PEN substrate (a), a Pt/Ti electrode (from PECCELL Technologies Inc.) (b) and a prepared Pt counter electrode on the ITO/PEN substrate (c). The ITO/PEN has no oxidation and reduction peak because the ITO/PEN cannot catalyze the redox couple regeneration of the triiodide ion. The prepared Pt counter electrode (Figure 3(c)) shows two pairs of oxidation and reduction peaks similar to those in the commercial Pt/Ti counter electrode (Figure 3(b)). The oxidation and reduction pair (peaks B_{ox} and B_{red}) on the right is attributed
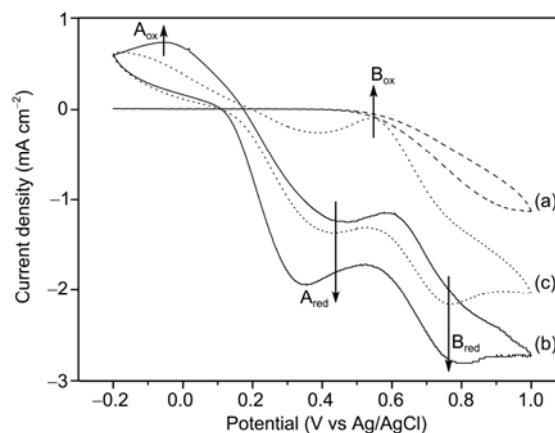
Figure 3   Cyclic voltammograms at a scan rate of 50 mV s^{-1} for (a) ITO/PEN, (b) a Pt/Ti electrode (from PECCELL Technologies), and (c) the prepared Pt counter electrode on the ITO/PEN substrate.

to the redox reaction of $I_3^-+2e^-\rightarrow 3I^-$,which directly affects the DSSC performance; while that (peaks A_{ox} and A_{red}) on the left resulted from the redox reaction of $3I_2+2e^-\rightarrow 2I_3^-$, which has little effect on the DSSC performance [23,24]. For this reason, the obtained Pt counter electrode has similar electrocatalytic activity for the I_3^-/I^- redox as the commercial Pt/Ti electrode.
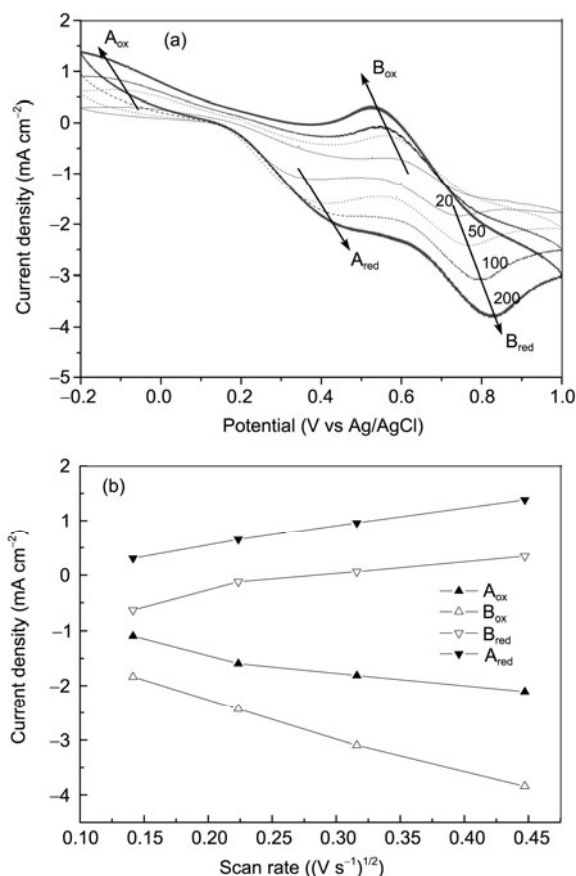
Repeated CVs of the fabricated Pt counter electrode (Figure 4(a)) demonstrate the peak positions and the current

densities scarcely change with successive scans. The redox peak currents show a good linear relationship with cycle times (Figure 4(b)), which indicates that the Pt film has good chemical stability. Figure 4(c) shows 200 successive CV cycles of the fabricated Pt counter electrode. On consecutive scans, the peak positions and current densities hardly change indicating the Pt particles were tightly bound to the ITO/PEN surface [25].

Figure 5(a) shows CVs of the I_3^-/I^- system with the fabricated Pt counter electrode at various scan rates. As expected the peak current densities change with different scan rates. The reduction peaks shift linearly to the negative and the corresponding oxidation peaks shift to the positive with increasing scan rates. Figure 5(b) illustrates a relationship between both the oxidation and reduction peak currents and the square root of the scan rate. The clear linear relationship at different scan rates indicates that the oxidation and reduction reaction are diffusion limited by the transport of iodide species away from the Pt counter electrode surface. This phenomenon suggests there is no specific interaction between the I_3^-/I^- redox couple and the Pt counter electrode as is desired, and is similar to that of the commercial Pt/Ti electrode. It shows that any adsorption of the iodide species

Figure 4 Repeated cyclic voltammograms of the I_3^-/I^- system with the fabricated Pt counter electrode at a scan rate of 50 mV s^{-1} for (a) 10 cycles, (b) a graph of redox peak currents at each cycle and (c) for 200 cycles.

Figure 5 (a) Cyclic voltammograms for the Pt counter electrode with different scan rates (from inner to outer: 20, 50, 100 and 200 mV s^{-1}, respectively), and (b) graph of the redox peak currents versus scan rates.

on the Pt counter electrode has little effect on the redox reaction [26,27].

2.3 Influence of the $H_2PtCl_6 \cdot 6H_2O$ content to form the Pt counter electrodes on the photoelectric properties

The photovoltaic performances of the flexible DSSCs fabricated with different $H_2PtCl_6 \cdot 6H_2O$ contents are summarized in Table 1. It shows that the Pt counter electrode fabricated with no $H_2PtCl_6 \cdot 6H_2O$ has little current density, fill factor and energy conversion efficiency, which is expected because the ITO/PEN cannot catalyze the redox couple regeneration of the triiodide ion. The remaining DSSCs have the same V_{OC} of 0.74 V. The V_{OC} is determined by the energy level difference between the Fermi level of the electron in TiO_2 and the redox potential of the electrolyte [1,2], and because these flexible DSSCs have the same compositions, their V_{OC} values are similar. However, the J_{SC} value first increases and then decreases with increasing $H_2PtCl_6 \cdot 6H_2O$ content, which is attributed to the counteracting electrocatalytic activity and light transmittance of the Pt counter electrode. As the $H_2PtCl_6 \cdot 6H_2O$ content increases, the electrocatalytic activity of the Pt counter electrode is enhanced; however, light transmittance is reduced, which results in a decrease in incident light harvest and photocurrent.

2.4 Influence of the heating treatment temperature and time to form the Pt counter electrodes on the photovoltaic properties of the flexible DSSCs

The photovoltaic performances of the flexible DSSCs fabricated with different heat treatments were measured and summarized in Table 2. It shows the J_{SC} and η values first
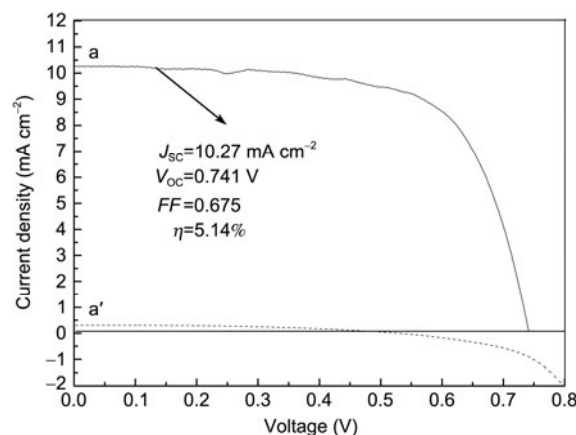
increase and then decrease with both increases in the temperature and time. Higher temperature and longer time result in the $H_2PtCl_6 \cdot 6H_2O$ being more completely decomposed, giving higher electrocatalytic activities. However, the higher heating temperature and longer heating time cause the damage to the PEN/ITO film, and the resistance in the substrate increases [28], which results in a decrease in the photocurrent and photovoltage in the DSSCs.

2.5 Photovoltaic performances of the flexible DSSC with the fabricated Pt counter electrode

Based on the optimized conditions, a Pt counter electrode was prepared by heating $H_2PtCl_6 \cdot 6H_2O$ (0.50wt%) at 120°C for 2 h in a vacuum oven, and a flexible DSSC was assembled. The photocurrent-voltage curve (Figure 6(a)) of the flexible DSSC was measured under a simulated solar light irradiation of 100 mW cm^{-2}. The energy conversion efficiency of the flexible DSSC with the fabricated Pt counter electrode reached 5.14%. The high photovoltaic performances of the flexible DSSC come from the counter electrode covered with enough Pt particles to give a large surface area on the electrode and excellent stability in the liquid electrolyte. It allows for an increase in the I_3^-/I^- redox reaction rate at the Pt counter electrode [26,29]. Therefore, the flexible DSSC with the fabricated Pt counter electrode has excellent photoelectric performance and stability. Figure 6(a)′ shows the dark current-voltage curve. It is obvious that the dark current for this cell is higher than that of the previously prepared DSSCs [4,6], which is due to no reaction between Ti foil and I_2. Therefore, improvements in the energy conversion efficiency for this cell could be ascribed to the inhibition of the reaction between the Ti substrate and I_2.

3 Conclusion

A Pt film was deposited on a flexible ITO/PEN substrate to

Table 1 Photovoltaic performances of the flexible DSSCs fabricated with different $H_2PtCl_6 \cdot 6H_2O$ contents

$H_2PtCl_6 \cdot 6H_2O$ content (%)	LT [a] (%)	J_{SC} (mA cm^{-2})	V_{OC} (V)	FF	η (%)
0	88	0.09	0.654	0.131	0.08
0.25	87	9.09	0.735	0.559	3.73
0.50	83	10.27	0.741	0.675	5.14
0.75	72	8.16	0.746	0.668	4.07

a) LT (Light Transmittance) was measured using a radiometer (FZ-A, Photoelectric Instrument of Beijing Normal University, China).

Table 2 Influence on the photoelectric properties of different temperature and time during the heat treatment

Time (min)	Temperature (°C)	J_{SC} (mA cm^{-2})	V_{OC} (V)	FF	η (%)
60	120	8.52	0.737	0.667	4.19
120	120	10.27	0.741	0.675	5.14
180	120	9.19	0.745	0.665	4.55
120	100	7.36	0.711	0.622	3.25
120	120	10.27	0.741	0.675	5.14
120	150	6.52	0.726	0.651	3.08

Figure 6 Current-voltage curves of the flexible DSSC with the fabricated Pt counter electrode.

form a flexible and transparent counter electrode by the vacuum thermal decomposition at a relatively low temperature. The Pt counter electrode has high electrocatalytic activity for the I_3^-/I^- system, good chemical stability and good light transmittance. After optimization, a Pt counter electrode was prepared by heating $H_2PtCl_6 \cdot 6H_2O$ (0.50 wt%) at 120°C for 2 h in a vacuum oven, the resultant flexible DSSC achieved a photoelectric energy conversion efficiency of 5.14% under a simulated solar light irradiation with intensity of 100 mW cm^{-2}. Compared with other methods of Pt counter electrodes preparation, vacuum thermal decomposition is simple and suitable for flexible polymer substrates. The high electrocatalytic activity for the I_3^-/I^- redox reaction allows the Pt counter electrode to be used in flexible DSSCs and other fields.

1 O' Regan B, Grätzel M. Low-cost high-efficiency solar cell based on dye-sensitized colloidal TiO₂ films. Nature, 1991, 353: 737–740
2 Grätzel M. Recent advances in sensitized mesoscopic solar cells. Acc Chem Res, 2009, 42: 1788–1798
3 Longo C, Freitas J, DePaoli M. Performance and stability of TiO₂/dye solar cells assembled with flexible electrodes and a polymer electrolyte. J Photochem Photobiol A: Chem, 2003, 159: 33–39
4 Xiao Y M, Wu J H, Li Q H, et al. Preparation of photoanode and its application to flexible dye-sensitized solar cells. Chin Sci Bull, 2010, 55: 980–985
5 Yue G T, Wu J H, Xiao Y M, et al. Flexible dye-sensitized solar cell based on PCBM/P3HT heterojunction. Chin Sci Bull, 2011, 56: 325–330
6 Xiao Y M, Wu J H, Yue G T, et al. The preparation of titania nanotubes and its application in flexibledye-sensitized solar cells. Electrochim Acta, 2010, 55: 4573–4578
7 Wang Y, Wu J H, Lan Z, et al. Preparation of porous nanoparticle TiO₂ films for flexible dye-sensitized solar cells. Chin Sci Bull, 2011, 56: 2649–2653
8 Grätzel M. Photoelectrochemical cells, Nature, 2001, 414: 338–344
9 Papageorgiou N. Counter-electrode function in nanocrystalline photoelectrochemical cell configurations. Coor Chem Rev, 2004, 248: 1421–1446
10 Hagfeldt A, Boschloo G, Sun L, et al. Dye-sensitized solar cells. Chem Rev, 2010, 110: 6595–6663
11 Ikegami M, Miyoshi K, Miyasak T. Platinum/titanium bilayer deposited on polymer film as efficient counter electrodes for plastic dye-sensitized solar cells. Appl Phys Lett, 2007, 90: 153122–153129
12 Grätzel M. High-efficiency (7.2%) flexible dye-sensitized solar cells with Ti-metal substrate for nanocrystalline-TiO₂ photoanode. Chem Commun, 2006, 38: 4004–4006
13 Kang M G, Park N G, Ryu K S, et al. A 4.2% efficient flexible dye-sensitized TiO₂ solar cells using stainless steel substrate. Sol Energy Mater Sol Cells, 2006, 90: 574–581
14 Park J H, Jun Y, Yun H G, et al. Fabrication of an efficient dye-sensitized solar cell with stainless steel substrate. J Electrochem Soc, 2008, 155: F145–F149
15 Chen L L, Tan W W, Zhang J B, et al. Fabrication of high performance Pt counter electrodes on conductive plastic substrate for flexible dye-sensitized solar cells. Electrochim Acta, 2010, 55: 3721–3726
16 Sun K, Fan B H, Ouyang J Y. Nanostructured platinum films deposited by polyol reduction of a platinum precursor and their application as counter electrode of dye-sensitized solar cells. J Phys Chem C, 2010, 114: 4237–4244
17 Takurou N, Murakami A, Grätzel M. Counter electrodes for DSC: Application of functional materials as catalysts. Inorg Chim Acta, 2008, 361: 572–580
18 Yuan Z, Su B. Titanium oxide nanotubes, nanofibers and nanowires, Colloids Surfaces A, 2004, 241: 173–183
19 Wu J H, Lan Z, Lin J M, Huang M L, et al. A novel thermosetting gel electrolyte for stable quasi-solid-state dye-sensitized solar cells. Adv Mater, 2007, 19: 4006–4011
20 Wu J H, Hao S C, Lan Z, et al. An all-solid-state dye-sensitized solar cell-based poly(N-alkyl-4-vinyl- pyridine iodide) electrolyte with efficiency of 5.64%. J Am Chem Soc, 2008, 130: 11568–11569
21 Lan Z, Wu J H, Hao S C, et al. Template-free synthesis of closed-microporous hybrid and its application in quasi-solid-state dye-sensitized solar cells. Energy Environ Sci, 2009, 2: 524–528
22 Grätzel M. Perspectives for dye-sensitized nanocrystalline solar cells. Prog Photovoltaic Res Applic, 2000, 8: 171–185
23 Huang Z, Liu X, Li K, et al. Application of carbon materials as counter electrodes of dye-sensitized solar cells. Electrochem Commun, 2007, 9: 596–598
24 Mei X, Cho S, Fan B, et al. High-performance dye-sensitized solar cells with gel-coated binder-free carbon nanotube films as counter electrode. Nanotechnology, 2010, 21: 395202–395209
25 Guo H, Li Y, Fan L, et al. Voltammetric behavior study of folic acid at phosphomolybdic-polypyrrole film modified electrode. Electrochim Acta, 2006, 51: 6230–6237
26 Saito Y, Kubo W, Kitamura T, et al. I⁻/I₃⁻ redox reaction behavior on poly(3,4-ethylenedioxythiophene) counter electrode in dye-sensitized solar cells. J Photochem Photobiol A: Chem, 2004, 164: 153–157
27 Biallozor S, Kupniewska A. Study on poly(3,4-ethylenedioxy thiophene) behaviour in the I⁻/I₂ solution. Electrochem Commun, 2000, 2: 480–486
28 Zhang D S, Yoshida T, Furuta K, et al. Hydrothermal preparation of porous nanocrystalline TiO₂ electrodes for flexible solar cells. J Photochem Photobiol A: Chem, 2004, 164: 159–166
29 Imoto K, Takahashi K, Yamaguchi T, et al. High-performance carbon counter electrode for dye-sensitized solar cells. Sol Energy Mater Sol Cells, 2003, 79: 459–469